

A DEEP LEARNING APPROACH TOWARDS PORE EXTRACTION FOR HIGH-RESOLUTION FINGERPRINT RECOGNITION

Hong-Ren Su, Kuang-Yu Chen, Wei Jing Wong, Shang-Hong Lai

Department of Computer Science, National Tsing Hua University, Taiwan

ABSTRACT

As high-resolution fingerprint images are becoming more common, the pores have been found to be one of the promising candidates in improving the performance of automated fingerprint identification systems (AFIS). This paper proposes a deep learning approach towards pore extraction. It exploits the feature learning and classification capability of convolutional neural networks (CNNs) to detect pores on fingerprints. Besides, this paper also presents a unique affine Fourier moment-matching (AFMM) method of matching and fusing the scores obtained for three different fingerprint features to deal with both local and global linear distortions. Combining the two aforementioned contributions, an EER of 3.66% can be observed from the experimental results.

Index Terms— High-resolution fingerprint recognition, pore extraction, convolutional neural network, affine Fourier moment-matching

1. INTRODUCTION

Conventional automated fingerprint identification systems (AFIS) utilize the level 1 and 2 features for fingerprint matching. With the current development of fingerprint sensor technology, high-resolution fingerprint images (≥ 1000 dpi) are more accessible now. With these images, finer fingerprint features (level 3 features) can be extracted and used for fingerprint matching to further enhance the recognition accuracy of AFIS. Among the level 3 fingerprint features observed [1], the pores have been found to yield high recognition capability.

Stosz and Alyea [2] pioneered in using pores for fingerprint authentication. The pores were extracted by tracking the skeletonized fingerprint image. Fingerprint matching incorporated both minutiae information and pore locations. Further improvement to this method was suggested from several aspects [1]. First, Gabor filter and wavelet transform were applied for better denoising effect in fingerprint image processing. Regions with high negative frequency response and within certain area size were taken as the pores. Furthermore, two different matchers were used for the matching of level 2 features, namely minutiae-based matcher and correlation-based matcher [3], and the pores were matched using the modified iterative closest point (ICP) algorithm [4] for better

robustness against poor quality images. Other researchers have also attempted high-resolution fingerprint matching by using pores and ridge information [5, 6].

A pore-based high-resolution fingerprint matching algorithm was proposed by Zhao et al. [7], where the pores were extracted using the adaptive pore model (APM) [8]. Each pore was converted into a feature vector through the proposed pore descriptor. The pore descriptor is translation- and rotation-invariant, hence eliminate the need for fingerprint alignment. Due to this advantage, the descriptor-based approach has become a major research direction in recent works [9, 10]. A pore filtering technique via spatial analysis [11] was then introduced to improve the performance of APM. Furthermore, matching corresponding pores through sparse representation and the weighted random sample consensus (WRANSAC) algorithm [12] was demonstrated [13]. Instead of using standard fingerprint features, SIFT points have been successfully amalgamated with pores in high-resolution fingerprint matching [14].

In this work, we introduce a novel approach towards fingerprint pore extraction. Most existing pore extraction methods either adopted the image intensity analysis approach [2, 6, 10] or the filter approach [1, 5, 7, 8, 9, 11, 13]. This work takes a completely different approach by using convolutional neural network (CNN) for pore extraction. To the best of our knowledge, there has not been any similar work published before. With a large training dataset, CNNs are able to extract appropriate features and perform classification simultaneously in high accuracy. The proposed pore extraction technique exploits such quality of CNNs to capture the distinctive features of pores. In addition, we use the affine Fourier moment-matching (AFMM) technique [15] for fingerprint matching. Unlike conventional metric-based matching, this method assumes an affine mapping exist between two fingerprints and computes the error based on Fourier moment-matching (FMM) algorithm.

2. PORE EXTRACTION

2.1. Problem Formulation

Since pores are small (surface area of 5 to 40 pixels in a 1200 dpi image), smaller patches of size $N \times N$ are extracted from

the original fingerprint image for individual pore recognition. Given an image patch \mathbf{I} , our goal is to use the CNN to predict whether it centers at a pore. This is a binary classification problem which can be formulated as

$$\hat{d} = \operatorname{argmax}_{d \in \{0,1\}} p(d|\mathbf{I}), \quad (1)$$

where $d = 1$ indicates the presence of pore in the image patch while $d = 0$ means otherwise. In any supervised learning-based algorithm, the probability model $p(d|\mathbf{I})$ is obtained through a training process provided the training patches \mathbf{I}_t and the corresponding labels \mathbf{L}_t . The prediction in (1) can then be rewritten as

$$\hat{d} = \operatorname{argmax}_{d \in \{0,1\}} p(d|\mathbf{I}; \mathbf{I}_t, \mathbf{L}_t). \quad (2)$$

2.2. CNN Architecture

There are several CNN models in the literature created for image classification, for example LeNet-5 [16], AlexNet [17], VGGNet [18] and GoogLeNet [19]. All of the aforementioned CNN models have a pre-defined input image size and specialize in either digit or object recognition. Although existing deep learning tools such as Caffe [20] allow fine-tuning of pre-trained CNNs to adapt to new classification problem, we have another task to complete — to find the neighbourhood size $N \times N$ that produces the optimal pore recognition accuracy. For this, we propose a CNN architecture that accepts input image with arbitrary size.

Fig. 1 shows the overall architecture of the proposed CNN used for pore recognition and extraction. The network consists of nine layers with weights, including the first seven convolutional layers and the last two fully-connected layers. Each convolutional layer contains a convolution operation followed by a rectified linear unit (ReLU) [17] and all of them share a standard set of hyperparameters. The filter size is set to 3×3 with a stride of 1. The advantage of using a stack of convolutional layers with smaller filters over one layer with larger filter of equivalent effective receptive field is that the former creates a deeper network and thus, is able to learn more discriminative features [18]. Furthermore, the number of weights can be drastically reduced in this way. The number of filters in the convolutional layers is set to $2^{\lceil l/2 \rceil + 5}$, where l represents the layer number.

The first fully-connected layer enables the network to learn the non-linearity among the spatial features, and has an output size of 4096. On the other hand, the final two-way fully-connected layer prepares the features for the succeeding softmax binary classification function.

During testing, the individual pore recognition task can be extended to the pore extraction of a full fingerprint image. However, since fully-connected layers are computed with matrix multiplication, the number of weights is heavily dependent on the output size of the previous layer, which is indirectly controlled by the input image size. In order to employ

the entire fingerprint image in the same network described above, the fully-connected layers have to be converted into convolutional layers [18]. It can be done by replacing a K -output fully-connected layer with a convolutional layer with K filters of size equivalent to the size of the feature maps in the previous layer. The output of the testing network is a binary map with 1's indicating the locations of pores.

3. FINGERPRINT MATCHING

3.1. Affine Fourier Moment-Matching

Considering two fingerprint images on the affine space $f_1(x, y)$ and $f_2(x', y')$, there exists an affine mapping between them described as

$$f_2(x', y') \mapsto \mathbf{A} f_1(x, y) + \mathbf{t}, \quad (3)$$

where (x, y) and (x', y') represents the coordinate systems in the two fingerprints, $\mathbf{A} = \begin{bmatrix} a_{11} & a_{12} \\ a_{21} & a_{22} \end{bmatrix} = \alpha \begin{bmatrix} \cos(\theta) & -\sin(\theta) \\ \sin(\theta) & \cos(\theta) \end{bmatrix}$ defines a linear transformation, and $\mathbf{t} = \begin{bmatrix} t_1 \\ t_2 \end{bmatrix}$ is the translation vector.

Assuming that the Fourier transforms of $f_1(x, y)$ and $f_2(x', y')$ are $F_1(u, v)$ and $F_2(u', v')$ respectively, it was shown [21] that

$$F_1(u, v) = \frac{1}{|\Delta|} \exp^{i(2\pi/\Delta)(t_1 u' + t_2 v')} F_2(u', v'), \quad (4)$$

with $\begin{bmatrix} u \\ v \end{bmatrix} = \begin{bmatrix} a_{11} & a_{12} \\ a_{21} & a_{22} \end{bmatrix} \begin{bmatrix} u' \\ v' \end{bmatrix}$ and $\Delta = \begin{vmatrix} a_{11} & a_{12} \\ a_{21} & a_{22} \end{vmatrix}$. By using the moment-matching method and least squares estimation, Su and Lai [15] derived the energy cost function between the second-degree Fourier moments of two affine-related images as

$$E(\mathbf{A}, \mathbf{t}) = \sum_{d=1}^2 w_d \|\mathbf{M}_d^{(1)} - \mathbf{C}_d \mathbf{M}_d^{(2)}\|^2 + \|f_2(\mathbf{A}, \mathbf{t}, x, y) - f_1(x, y)\|^2 \quad (5)$$

where d is the degree of moment, w_d is the weight associated with the d -th degree Fourier moment constraint, \mathbf{C}_d is the coefficient matrix of the d -th degree moment, and $\mathbf{M}_d^{(1)}$ and $\mathbf{M}_d^{(2)}$ are the d -th degree moments for the two images respectively. The definitions for \mathbf{C}_d , $\mathbf{M}_d^{(1)}$ and $\mathbf{M}_d^{(2)}$ follow those described in [15] and are omitted in this paper.

3.2. Fingerprint Matching using AFMM

In the proposed work, we use all three levels of features for high-resolution fingerprint matching, namely the ridge pattern, minutiae and pores. The ridge pattern and minutiae are extracted using wavelet-based Gabor filtering [22] and the crossing number algorithm [23]. Each level of these features

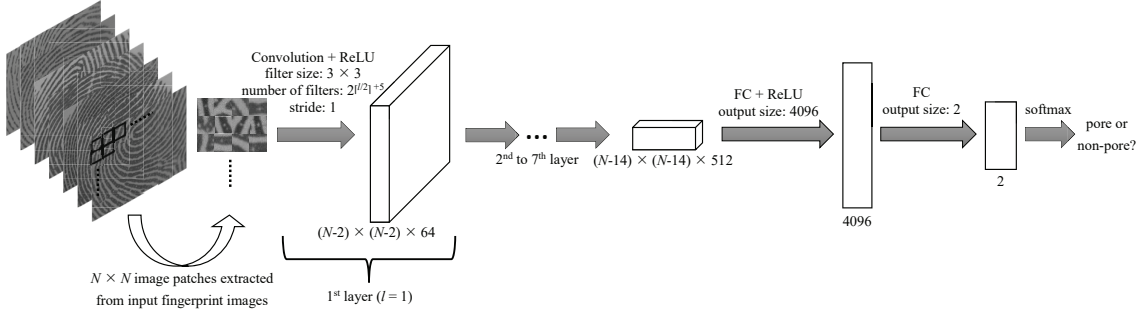


Fig. 1. The architecture of the proposed CNN.

is represented as a binary map and the error between two maps can be expressed with (5). Hence, the error between two fingerprints is derived as

$$E_F(\mathbf{A}, \mathbf{t}) = E_R(\mathbf{A}, \mathbf{t}) + E_M(\mathbf{A}, \mathbf{t}) + E_P(\mathbf{A}, \mathbf{t}), \quad (6)$$

where $E_R(\mathbf{A}, \mathbf{t})$, $E_M(\mathbf{A}, \mathbf{t})$ and $E_P(\mathbf{A}, \mathbf{t})$ are the error contributions from matching ridge pattern, minutiae and pores respectively.

Regardless of whether it is a genuine or an impostor matching, the objective is to minimize the error with respect to a set of affine mapping parameters \mathbf{A} and \mathbf{t} , that is, to compute $\min_{\mathbf{A}, \mathbf{t}} E_F$. In this paper, the gradient descent method is used to solve this optimization problem. In the context of fingerprint matching, we are trying to find the mapping in (3) that best describes the affine relationship between two fingerprints with error E_F . The error can be used as the distance measure for matching two fingerprints.

The method described above compares two fingerprints globally (AFMM-G). To improve the robustness against local distortions, the block-wise AFMM matching algorithm (AFMM-B) as shown in Fig. 2, is proposed. First, the query fingerprint is divided into 12 non-overlapping blocks of the same size. For each block, a sliding window is created to iterate through the registered fingerprint and find the block with the lowest error. A voting scheme is then set up to record the number of matchable blocks, S . A block is said to be matchable if it corresponds to another block in the registered fingerprint with error less than a pre-defined threshold ($E_{F,i} < \tau$, where i represents the block number). S is taken as the final matching score between two fingerprints. τ is set to 0.7 in this paper.

4. EXPERIMENTAL RESULTS AND ANALYSIS

4.1. Accuracy of Pore Extraction

In this work, we use PolyU HRF DBI [24] for experiments. The 30 fingerprint images with ground truth of pores were used to evaluate the pore extraction method. The first 20 images were used for training while the remaining for testing.

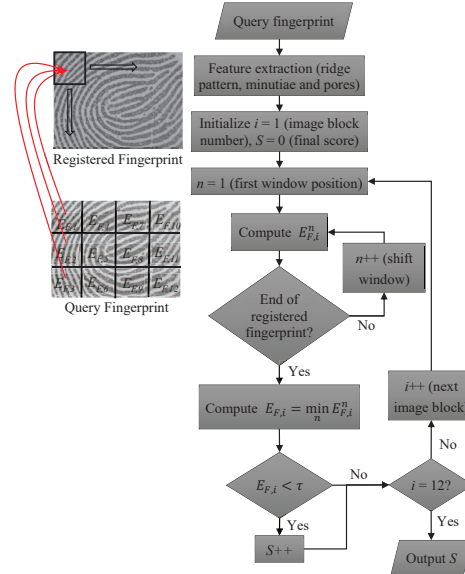


Fig. 2. Visual illustration and flow chart of the proposed AFMM-B algorithm.

For training, a $N \times N$ image patch is extracted from each of the pixel on the fingerprint images. If a image patch is centered within 3 pixels from the given ground truth of pore positions, it is labeled as 1; otherwise 0. There are approximately 2.6 millions patches used for training.

Table 1 shows the pore detection rates of the proposed CNN-based pore extraction method with different patch sizes. As pores are located on ridges, it is ideal for an image patch to include the pore, and the surrounding ridge and valley so that the CNN has sufficient information to identify the pattern of a pore. Results indicate $N = 17$ outperforms other patch sizes with 88.6% of true detection rate (TDR). It means that the proposed CNN architecture in Fig. 1 can best recognize a pore given its 17×17 neighbourhood on the fingerprint image. The proposed pore extraction method also shows comparable results to the existing methods with significantly low false detection rate (FDR). We use the following definitions



Fig. 3. Examples of the pores detected by the proposed CNN-based pore extraction method. TP predictions are denoted by red circles, while FP predictions are green squares.

for TDR and false detection rate (FDR) to consider the accuracy of positive (pores) detection.

$$TDR = \frac{TP}{\text{total number of true pores}}; \quad (7)$$

$$FDR = \frac{FP}{\text{total number of true pores}}, \quad (8)$$

where TP and FP represents the number of correctly and falsely predicted pores, respectively. Fig. 3 illustrates the resulting TP and FP predictions of the proposed method.

Table 1. Experimental results of the proposed and other existing pore extraction methods. The detection rates of existing methods reflect the results reported in the corresponding papers.

Method		TDR	FDR
Proposed	$N = 15$	84.4%	0.8%
CNN-based	$N = 17$	88.6%	0.4%
method	$N = 19$	83.1%	0.9%
Pamplona Segundo et al. [6]		90.8%	11.1%
Teixeira et al. [11]		86.1%	8.6%
Zhao et al. [9]		84.8%	17.6%
Jain et al. [1]		75.9%	23.0%

4.2. Performance of Fingerprint Recognition

The full testing set of DBI was used for fingerprint recognition performance evaluation. It consists of 1480 high-resolution partial fingerprint images from 148 subjects with 10 samples per subject. The experiment in this sub-section was performed based on $N = 17$.

As shown in Table 2, the equal-error rate (EER) of the proposed high-resolution fingerprint recognition method is comparable to that of the state-of-the-art methods. First of all, it has been shown in Section 4.1 that the proposed CNN-based pore extraction method yields high accuracy. Having this advantage, complemented with the invariant properties of the proposed AFMM-based fingerprint matching method, the EER obtained is as low as 3.66%.

Table 2. Performance of the proposed high-resolution fingerprint recognition algorithm and other existing methods as reported in the original papers.

Method	EER
AFMM-G (with pores)	4.67%
AFMM-B (with pores)	3.66%
AFMM-B (without pores)	13.26%
Pamplona Segundo et al. [6]	3.74%
Cui et al. [10]	10.46%
de Assis Angeloni et al. [5]	22.30%
Liu et al. [13]	5.41%
Jain et al. [1]	30.45%

From the table, it is notable that AFMM-B is more superior than AFMM-G. AFMM-B matches fingerprints locally to address regional distortions that occur due to uneven pressure applied on the fingerprint scanner, whereas AFMM-G produces only one global set of affine mapping parameters to conclude the transformation between two fingerprints. Furthermore, if the pores information is excluded from the matching process, the EER is increased by 9.6%. This proves that the pores play a crucial role in high-resolution fingerprint matching, especially for partial fingerprint images, where limited ridge pattern and minutiae are available.

5. CONCLUSIONS

In this paper, we presented a new pore extraction approach based on deep learning. Specifically, we designed and trained a CNN model to recognize pores in a small image block. Taking advantage of the feature learning capability of CNNs, the proposed method was able to achieve a pore detection rate of 88.6%. We also introduced the idea of using AFMM in high-resolution fingerprint matching, which fuses the scores of matching ridge pattern, minutiae and pores. Experimental results showed that the proposed method yields recognition accuracy comparable to the state-of-the-art methods. As this work demonstrated the potential of using deep learning for pore extraction, the future work is to design and consolidate an application-specific deep learning architecture to further elevate the performance. Another future work is to develop a high-resolution fingerprint recognition framework that better utilizes the three levels of features.

6. ACKNOWLEDGEMENT

This work was supported by Novatek Microelectronics Corporation (project code: 105F8005EA).

7. REFERENCES

- [1] A.K. Jain, Y. Chen, and M. Demirkus, “Pores and ridges: High-resolution fingerprint matching using level 3 features,” vol. 29, no. 1, pp. 15–27, 2007.
- [2] J.D. Stosz and L.A. Alyea, “Automated system for fingerprint authentication using pores and ridge structure,” in *SPIE’s 1994 International Symposium on Optics, Imaging, and Instrumentation*. International Society for Optics and Photonics, 1994, pp. 210–223.
- [3] A.K. Jain, S. Prabhakar, and S. Chen, “Combining multiple matchers for a high security fingerprint verification system,” *Pattern Recognit. Lett.*, vol. 20, no. 11, pp. 1371–1379, 1999.
- [4] P.J. Best and N.D. McKay, “A method for registration of 3-d shapes,” vol. 14, no. 2, pp. 239–256, 1992.
- [5] M. de Assis Angeloni and A.N. Marana, “Improving the ridge based fingerprint recognition method using sweat pores,” in *Proceedings of the Seventh International Conference on Digital Society*, 2013.
- [6] M. Pamplona Segundo and R. de Paula Lemes, “Pore-based ridge reconstruction for fingerprint recognition,” in *Proceedings of the IEEE Conference on Computer Vision and Pattern Recognition Workshops*, 2015, pp. 128–133.
- [7] Q. Zhao, L. Zhang, D. Zhang, and N. Luo, “Direct pore matching for fingerprint recognition,” in *Advances in Biometrics*, pp. 597–606. Springer, 2009.
- [8] Q. Zhao, L. Zhang, D. Zhang, N. Luo, and J. Bao, “Adaptive pore model for fingerprint pore extraction,” in *Pattern Recognition, 2008. ICPR 2008. 19th International Conference on*. IEEE, 2008, pp. 1–4.
- [9] Q. Zhao, D. Zhang, L. Zhang, and N. Luo, “High resolution partial fingerprint alignment using pore–valley descriptors,” *Pattern Recognition*, vol. 43, no. 3, pp. 1050–1061, 2010.
- [10] J. Cui, M.-S. Ra, and W.Y. Kim, “Fingerprint pore matching method using polar histogram,” in *The 18th IEEE International Symposium on Consumer Electronics (ISCE 2014)*. IEEE, 2014, pp. 1–2.
- [11] R.F.S. Teixeira and N.J. Leite, “Improving pore extraction in high resolution fingerprint images using spatial analysis,” in *2014 IEEE International Conference on Image Processing (ICIP)*. IEEE, 2014, pp. 4962–4966.
- [12] D. Zhang, W. Wang, Q. Huang, S. Jiang, and W. Gao, “Matching images more efficiently with local descriptors,” in *Pattern Recognition, 2008. ICPR 2008. 19th International Conference on*. IEEE, 2008, pp. 1–4.
- [13] F. Liu, Q. Zhao, L. Zhang, and D. Zhang, “Fingerprint pore matching based on sparse representation,” in *ICPR 2010*, 2010, pp. 1630–1633.
- [14] S. Malathi and C. Meena, “Improved partial fingerprint matching based on score level fusion using pore and sift features,” in *Process Automation, Control and Computing (PACC), 2011 International Conference on*. IEEE, 2011, pp. 1–4.
- [15] H.-R. Su and S.-H. Lai, “Non-rigid registration of images with geometric and photometric deformation by using local affine fourier-moment matching,” in *Proceedings of the IEEE Conference on Computer Vision and Pattern Recognition (CVPR)*, 2015, pp. 2874–2882.
- [16] Y. LeCun, B. Boser, J.S. Denker, D. Henderson, R.E. Howard, W. Hubbard, and L.D. Jackel, “Backpropagation applied to handwritten zip code recognition,” *Neural Comput.*, vol. 1, no. 4, pp. 541–551, 1989.
- [17] A. Krizhevsky, I. Sutskever, and G.E. Hinton, “Imagenet classification with deep convolutional neural networks,” in *Advances in neural information processing systems*, 2012, pp. 1097–1105.
- [18] K. Simonyan and A. Zisserman, “Very deep convolutional networks for large-scale image recognition,” *arXiv preprint arXiv:1409.1556*, 2014.
- [19] C. Szegedy, W. Liu, Y. Jia, P. Sermanet, S. Reed, D. Anguelov, D. Erhan, V. Vanhoucke, and A. Rabinovich, “Going deeper with convolutions,” in *Proceedings of the IEEE Conference on Computer Vision and Pattern Recognition (CVPR)*, 2015, pp. 1–9.
- [20] Y. Jia, E. Shelhamer, J. Donahue, S. Karayev, J. Long, R. Girshick, S. Guadarrama, and T. Darrell, “Caffe: Convolutional architecture for fast feature embedding,” in *Proceedings of the 22nd ACM international conference on Multimedia*. ACM, 2014, pp. 675–678.
- [21] R.N. Bracewell, K.-Y. Chang, A.K. Jha, and Y.-H. Wang, “Affine theorem for two-dimensional fourier transform,” *Electron. Lett.*, vol. 29, no. 3, pp. 304, 1993.
- [22] W.-P. Zhang, Q.-R. Wang, and Y.Y. Tang, “A wavelet-based method for fingerprint image enhancement,” in *Machine Learning and Cybernetics, 2002. Proceedings. 2002 International Conference on*. IEEE, 2002, vol. 4, pp. 1973–1977.
- [23] B.M. Mehtre, “Fingerprint image analysis for automatic identification,” *Mach. Vis. Appl.*, vol. 6, no. 2–3, pp. 124–139, 1993.
- [24] “PolyU HRF Database,” http://www4.comp.polyu.edu.hk/~biometrics/HRF/HRF_old.htm.